Chemical Research in Toxicology®

In Vitro and in Vivo Studies of the Electrophilicity of Physcion and its Oxidative Metabolites

Xiaotong Qin, Ying Peng, and Jiang Zheng

Chem. Res. Toxicol., **Just Accepted Manuscript** • DOI: 10.1021/acs.chemrestox.8b00026 • Publication Date (Web): 18 Apr 2018

Just Accepted

ACS Publications

is published by the American Chemical Society. 1155 Sixteenth Street N.W., Washington, DC 20036

In Vitro and *in Vivo* Studies of the Electrophilicity of Physcion and its Oxidative Metabolites

Xiaotong Qin,† Ying Peng,†* and Jiang Zheng†§*

†Wuya College of Innovation, Shenyang Pharmaceutical University, Shenyang, Liaoning, 110016, P.R. China

§State Key Laboratory of Functions and Applications of Medicinal Plants, Key Laboratory of Pharmaceutics of Guizhou Province, Guizhou Medical University, Guiyang, Guizhou, 550025, P.R. China

Corresponding Authors:

Jiang Zheng, PhD
Wuya College of Innovation, Shenyang Pharmaceutical University, No. 103, Wenhua Road, Shenyang, Liaoning, 110016, P. R. China
State Key Laboratory of Functions and Applications of Medicinal Plants, Key Laboratory of Pharmaceutics of Guizhou Province, Guizhou Medical University, 9 Beijing Road, Guiyang, Guizhou, 550025, P.R. China
Email: zhengneu@yahoo.com
Tel: +86-24-23986361; Fax: +86-24-23986510

Ying Peng, PhD
Wuya College of Innovation, Shenyang Pharmaceutical University, No. 103, Wenhua Road, Shenyang, Liaoning, 110016, P. R. China
Email: yingpeng1999@163.com
Tel: +86-24-23986361; Fax: +86-24-23986510

TOC graph

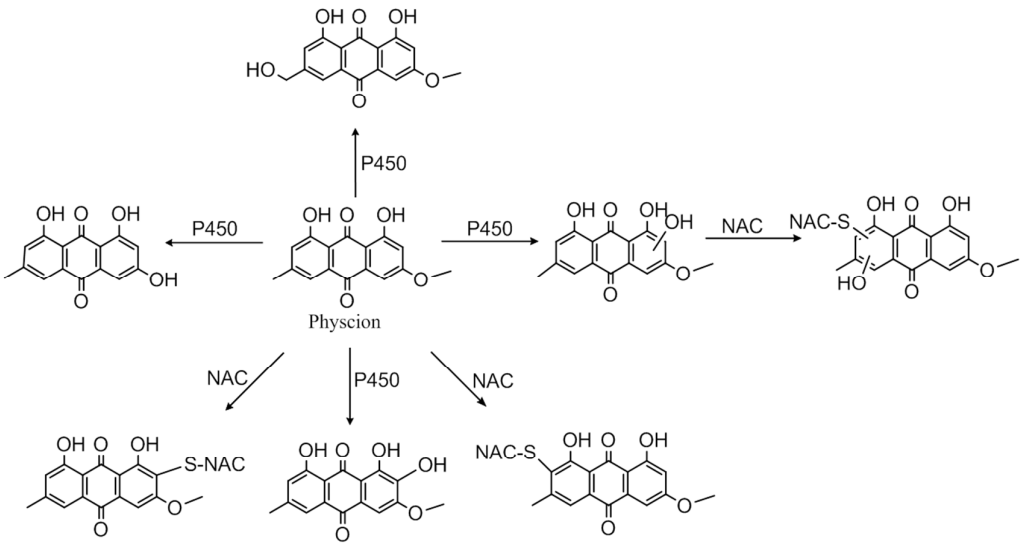

Abstract

Physcion (1,8-dihydroxy-3-methoxy-6-methyl-9,10-anthracenedione) is a bioactive component found in Polygoni Multiflori Radix (PMR) which has been widely used as traditional Chinese medicine. Unfortunately, studies showed hepatotoxicity of PMR during its clinical use. The mechanisms of its toxic action remain unknown. The major objectives of this study were to characterize oxidative metabolites of physcion *in vitro* and *in vivo* and to determine the electrophilicity of the parent compound and its oxidative metabolites**.** Five oxidative metabolites (M1–M5) were detected in rat liver microsomal incubations after exposure to physcion, and the formation of the metabolites was NADPH dependent. M1–M4 were mono-hydroxylation metabolites, and M5 was *O*-demethylation metabolite. A total of three *N*-acetylcysteine (NAC) conjugates (M6–M8) were observed in rat liver microsomes fortified with NAC as a trapping agent. M6 was derived from M4 conjugated with a molecule of NAC; M7 and M8 originated from parent compound physcion adducted with a molecule of NAC, respectively. M1–M8 were also observed in urine of rats given physcion. HLM incubations produced four oxidative metabolites and two NAC conjugates. The structures of M3, M7 and M8 were characterized by LC-Q-TOF MS and NMR. Recombinant P450 enzyme incubations demonstrated that CYPs2C19, 1A2, 2B6, and 3A4 were mainly involved in hydroxylation of physcion. The metabolism study assisted us to better understand the mechanisms of physcion-induced hepatotoxicity.

Introduction

Polygonum multiflorum Thunb., known as Heshouwu in China and Fo-ti in North America,[1] is an important Chinese herbal medicine and is officially listed in the Chinese Pharmacopoeia. Pharmacological studies and clinical practice demonstrated that it possesses anti-aging, anti-oxidative, anti-inflammatory, and anti-cancer effects.[2] In addition, it also exhibits effective outcome in the treatment of premature greying of hair, lumbago, spermatorrhea, leucorrhea and constipation.[3] Meanwhile, phytochemical studies shown that anthraquinones (AQs) are one of main bioactive components in *Polygonum multiflorum* Thunb..[4] In addition to their anti-bacterial properties, AQs exert anti-fungal and anti-cancer effects[3] and are considered to be useful for the disintegration and elimination of urinary stones.[5] However, with chronically used of Polygoni Multiflori Radix (PMR), the roots of *Polygonum multiflorum* Thunb., hepatic adverse effect were constantly reported since 1990s in China[6-9] and other countries.[10-17] Acute hepatitis was the most frequently reported hepatic adverse effect.[18-19] Since many AQ-containing herbal medicines have been reported to induce hepatic damages, AQs are assumed to be responsible for the observed hepatotoxicity.[20-21]

Physcion (1,8-dihydroxy-3-methoxy-6-methyl-9,10-anthracenedione), an AQ derivative, has been isolated and characterized from both terrestrial and marine sources.[22-24] In particular, physcion is rich in PMR which is widely used as traditional Chinese medicine. Physcion reportedly possessed the efficacies of anti-inflammatory,[25] anti-microbial,[26] and antineuroectodermal tumor properties.[27-28]

Physcion was found to be cytotoxic in HeLa, A549, HL-60, and SW680 cells.[29]

To our best knowledge, the causal link between physcion and its hepatic lesions, along with exact metabolic pathway of physcion, remains uncertain. The present study was undertaken to investigate (1) biotransformation of physcion *in vitro* and *in vivo* and (2) the electrophilicity of physcion and its metabolites possibly related with the observed cytotoxicity.

EXPERIMENTAL PROCEDURES

Chemicals and Materials. Physcion and emodin with purity of >98% were supplied by Chengdu Pufeide Biologic Technology Co. Ltd. (Chengdu, China). *N*-Acetylcysteine (NAC), nicotinamide adenine dinucleotide phosphate reduced (NADPH) and propranolol were obtained from Sigma-Aldrich (St. Louis, MO). Human liver microsomes (HLMs) and recombinant human P450 enzymes were purchased from BD Gentest (Woburn, MA). Rat (Sprague−Dawley, male) liver microsomes (RLMs) were prepared in our laboratory, according to a previously published method[30]. All organic solvents were acquired from Fisher Scientific (Springfield, NJ). Distilled water was purchased from Wahaha Co. Ltd. (Hangzhou, China). All of the reagents and solvents were analytical or high-performance liquid chromatography grade.

Microsomal Incubations. A stock solution of physcion was prepared in dimethyl sulfoxide (DMSO). The incubation mixtures were prepared in a final volume of 250 μL, containing 1.0 mg/mL RLM or HLM protein, 3.2 mM $MgCl_2$, 20 mM NAC, and 25 μM physcion. The microsomal reactions were initiated by adding NADPH (1.0 mM) and conducted at 37 °C in a gentle shaking water bath for 30 min. The negative control without NADPH was included to ensure that the metabolism of physcion was NADPH dependent. The reactions were quenched with an equal volume of ice-cold acetonitrile, followed by vortex-mixing and centrifuging at 19,000 *g* for 10 min to remove precipitated protein. A 5 μL aliquot of supernatants was

injected into an LC–MS/MS system for analysis. All incubations were carried out in duplicate.

Chemical Synthesis of Physcion Metabolites. The methyl moiety of physcion was oxidized to prepare M1, based on a reported procedure.[31] Briefly, physcion (40 mg) was dissolved in acetic acid (1 mL), followed by addition of acetic anhydride (1.8 mL) and concentrated sulfuric acid (18 μL) dropwise. The resulting mixture was stirred at 70 °C for 30 min and poured onto ice water to afford crystals of 1,3-diacetylphyscion. With the crude products (25 mg) dissolved in a mixture of glacial acetic acid (1 mL) and acetic anhydride (1 mL), an acetic acid solution (5 mL) containing chromium (VI) oxide (CrO_3, 600 mg) was dropwise added. The mixtures were stirred for 24 h at room temperature, whereafter, blown dried under a nitrogen stream and re-dissolved in dry tetrahydrofuran (THF) (500 μL). Borane-methylsulfide complex (175 μL) was added to the THF precooled at 0 °C. The reaction mixtures were further stirred at 0 °C for 1 h, and the reaction was terminated by mixing with water (1 mL). The resulting mixture was extracted with ethyl acetate, and the extracts were washed with 5% $NaHCO_3$ aqueous solution, followed by addition of 1 mL of potassium hydroxide solution (0.2 M). The mixture was stirred at 75 °C for 15 min. The resultant mixture was acidified and extracted with ethyl acetate, and the organic solvent was evaporated to acquire M1.

M2 was prepared by hydroxylation of physcion using boric acid, according to a reported procedure.[32] Briefly, physcion (10 mg) was mixed with 1 mL of 65%

oleum including boric acid (50 mg) in a sealed flask. The mixture was stirred at room temperature for 6 h and then was allowed to stand for 3 days. The solution was poured cautiously onto ice (25 g), followed by boiling for 10 min and chilling to room temperature. The resulting orange precipitates were harvested and then dissolved in 20 mL of 0.2 M potassium hydroxide solution under nitrogen. The mixture was heated on a boiling water bath for 15 min and the acidified with 5 mL of 5% HCl solution. The acidic solution was extracted with ethyl acetate (5 mL×3), and the organic phase was washed with H_2O (5 mL×3) and concentrated by evaporating under vacuum. The residue was recrystallized from dilute acetic acid and submitted to the LC-MS/MS analysis.

M3 and M4 were obtained from hydroxylation of physcion by a published protocol.[32] In brief, physcion (40 mg) and potassium persulfate (104 mg) were dissolved in sulfuric acid (2 mL). After being shaken for 10 min at room temperature, 104 mg potassium persulfate was added with stirring. After 45 min, the reaction was terminated by addition of 40 mL of water and 400 mg sodium metabisulfite. The mixture was extracted with butanol (6 mL) and washed with 5% HCl (20 mL) then water (20 mL). The solvent was evaporated and the residue was subjected to the LC-MS/MS system for analysis. Finally, M3 was purified by a semi-preparative HPLC system and characterized by mass spectrometry and NMR. ^{1}H-NMR (DMSO-d_6, 600 MHz): δ7.11 (1H, s, H-7), 7.34 (1H, s, H-4), 7.49 (1H, d, J=1.58 Hz, H-5).

NAC conjugates M7 and M8 were synthesized by direct reaction of NAC with

physcion. Physcion and NAC were dissolved in potassium phosphate buffer (pH = 7.4) and stirred at 37 °C for 2 h. The resultant mixture was concentrated by rotary evaporation and reconstituted with the initial mobile solvent and submitted to LC-MS/MS analysis. M7 and M8 were purified by a semi-preparative HPLC system and characterized by mass spectrometry and NMR. M7: ^{1}H NMR (DMSO-d_6, 600 MHz): δ2.42 (3H, s, H-11), 4.01 (3H, s, H-12), 7.19 (1H, s, H-7), 7.27 (1H, s, H-4), 7.52(1H, s, H-5); ^{13}C NMR (DMSO-d_6, 600 MHz): δ21.50 (C-11), 56.81 (C-12), 102.10 (C-4), 110.60 (C-9a), 113.60 (C-8a), 116.60 (C-2), 120.40 (C-5), 124.40 (C-7), 132.70 (C-4a), 133.80 (C-10a), 148.60 (C-6), 159.60 (C-1), 161.60 (C-8), 165.40 (C-3), 181.50 (C-10) 189.90 (C-9); M8: ^{1}H NMR (DMSO-d_6, 600 MHz): δ6.87 (1H, d, J=2.26 Hz, H-2), 7.18 (1H, d, J=2.33 Hz H-4), 7.53 (1H, s, H-5).

Synthetic products were purified on a YMC-Pack ODS-A column (250×10 mm, S-5, 12 nm) (YMC Co., Ltd, Japan), and the purification was achieved on a semi-preparative HPLC system. The rate was set 2.5 mL/min.

Animal Experiments. All animal manipulations met the requirements approved by the Ethics Review Committee for Animal Experimentation of Shenyang Pharmaceutical University (Shenyang, China). Male Sprague-Dawley rats (200±20 g) were obtained from the Animal Center of Shenyang Pharmaceutical University and were kept in a controlled environment (temperature of 25 °C and 12 h dark/light cycle) with maintaining on standard metabolism cages. Blank urine samples carefully conserved on ice were collected after a 12-h overnight with free access to water prior

to the treatment. Physcion dissolved in corn oil (13.6 mg/mL) were administered intraperitoneally at 75 mg/kg. Urine samples carefully preserved on ice were collected during the time periods of 0–12, 12–24, and 24–48 h after the procedure. During the experiments, the rats were allowed unlimited access to food and water. The collected urine samples were stored at -80 °C until analysis.

Sample Preparation for LC–MS/MS Analysis. Triple volumes of acetonitrile were added to the urine samples and the mixtures were vortexed for 3 min and centrifuged at 19,000 *g* for 10 min. The supernatants were collected and concentrated under a nitrogen flow at 40 °C. The resulting concentrates were reconstituted with 10% acetonitrile in water (100 μL) and centrifuged at 19,000 *g* for 10 min. A 3 μL aliquot of the supernatants was injected into the LC-MS/MS for analysis.

Recombinant Human P450 Enzyme Incubations. Physcion was individually incubated with nine recombinant human P450 enzyme (100 nM), including P450s 1A2, 2A6, 2B6, 2C9, 2C19, 2D6, 2E1, 3A4, and 3A5. Other conditions were equivalent to the microsomal incubation experiments. An equal volume of ice-cold acetonitrile which contained propranolol (40 ng/mL) as internal standard was mixed with incubation fluid to terminate the reactions. After vortexed for 2 min, the resulting samples were centrifuged at 16,000 *g* for 10 min. The supernatants (5 μL) were injected into the LC-MS/MS for analysis. Each incubation was carried out in duplicate. A total normalized rate method was applied. The rates of metabolite

formation in individual incubations with recombinant P450 enzymes were multiplied by the mean specific content of the corresponding P450 enzyme in HLMs to obtain the normalized reaction rates of each enzyme.[33]

LC-MS/MS Method. All samples were analyzed on an AB SCIEX Instruments 5500 triple quadrupole mass spectrometer (Applied Biosystems, Foster City, CA, USA) interfaced online with a 1260 infinity system (Agilent Technologies, Santa Clara, CA). The metabolite separation was achieved on an Accuore C_{18} column (4.6 × 150 mm, 5 μm; Waters, Ireland). Gradient elution was performed with acetonitrile containing 0.1% formic acid (solvent A) and 0.1% formic acid in water (solvent B) as follow: 10 % A at 0−2 min; 10−95 % A at 2−12 min; 95−95 % A at 12−17 min; 95−10 % A at 17−18 min; and 10−10 % A at 18−20 min. The flow rate was kept at 0.8 mL/min. The samples were analyzed in positive-ion mode with multiple-reaction monitoring (MRM) scanning. After tuning, the optimized MS instrument parameters were set at the following values: ion spray voltage (IS), entrance potential (EP) and ion source temperature were 5,500 V, 10 V, and 650 °C respectively; ion source gas 1, 50 psi; ion source gas 2, 50 psi; curtain gas, 35 psi. To achieve the highest sensitivity possible, MRM was used to selectively monitor with ion transitions (corresponding to declustering potential DP, collision energy CE) *m/z* 301→199 (100, 45) for hydroxylation metabolites, *m/z* 271→197 (100, 45) for *O*-demethylation metabolite, *m/z* 446→315 (100, 40) and 462→333 (100, 20) for NAC conjugates, *m/z* 260→116 (77, 25) for propranol (internal standard), and *m/z*

285→168(77, 25) for physcion.

In addition, a 1260 infinity LC system (Agilent Technologies, Boblingen, Germany) with an AB SCIEX 4000 Q-Trap MS (Applied Biosystems, Foster City, CA) were applied to trigger the enhanced product ion (EPI) scans by analyzing MRM signals which intended to gain abundant fragmentation information for target compounds. By using information-dependent acquisition (IDA) to trigger acquisition of EPI spectra for ions exceeding 1000 cps with exclusion of former target ions after three occurrences for 10 s. EPI scan was run in positive mode at a scan range of product ions from *m/z* 50 to 310 or 50 to 500. All data were processed using the AB SCIEX Analyst 1.6.2 software (Applied Biosystems).

RESULTS

Mass Spectrometric Behavior of Physcion. To facilitate the characterization of physcion metabolites, the chromatographic and mass spectrometric properties of parent compound were determined as an initial step. Positive mode was employed throughout the study, because of the higher sensitivity, ionization efficiency and more fragment ions obtained. Physcion showed fragment ions of *m/z* 239 ($[M+H-H_2O-CO]^+$), 211 ($[M+H-H_2O-2CO]^+$), 183 ($[M+H-H_2O-3CO]^+$), 252 ($[M+H-H_2O-CH_3]^+$), 242 ($[M+H-CO-CH_3]^+$), 196 ($[M+H-H_2O-2CO-CH_3]^+$), 168 ($[M+H-H_2O-3CO-CH_3]^+$), and 140 ($[M+H-H_2O-4CO-CH_3]^+$), along with $[M+H]^+$ as *m/z* 285 (Fig. 1), which results from the loss of CH_2O_2, $C_2H_2O_3$, $C_3H_2O_4$, CH_5O, C_2H_3O, $C_3H_5O_3$ $C_4H_5O_4$ and $C_5H_5O_5$ respectively.

In Vitro Oxidation of Physcion. Physcion was incubated in RLMs fortified with NADPH and NAC, and five oxidative metabolites (M1–M5) (Fig. 2B, 5B) and three NAC conjugates (M6–M8) were detected (Fig. 6B, 7B). Noteworthy, M7 and M8 were found in RLM incubations with or without NADPH (Fig. 7A, 7B), while no M1-M6 were observed when NADPH was absent in microsomal incubations (Fig. 2A, 5A, 6A). This indicates that the information of M1-M6 was NADPH-dependent.

Metabolites M1-M4 were oxidative metabolites of physcion. Formation of M1-M4 was monitored by acquiring precursor/product ion pair *m/z* 301/199 in positive mode. M1-M4 eluted out at retention time of 11.0, 12.3, 12.7, and 13.5 min, respectively (Fig. 2B). With MRM–EPI scanning (ion transition *m/z* 301/199), the

MS/MS spectra of M1-M4 were gained, which showed characteristic fragment ions of *m/z* 184 ($[MH\text{-}H_2O\text{-}3CO\text{-}CH_3]^+$), 199 ($[MH\text{-}H_2O\text{-}3CO]^+$), 212 ($[MH\text{-}H_2O\text{-}2CO\text{-}CH_3]^+$), 227 ($[MH\text{-}H_2O\text{-}2CO]^+$), and 255 ($[MH\text{-}H_2O\text{-}CO]^+$) (Fig. 3C, 3D, 4B, 4C). It is worth mentioning that the product ions of *m/z* 184, 199, 212, 227, and 255 were 16 Da more than the corresponding ions at *m/z* 168, 183, 196, 211, and 239 found in mass spectrum of the parent compound, indicating that M1-M4 were mono-hydroxylation metabolites of physcion. M1-M4 shared the same molecular ion at *m/z* 301, along with similar fragment patter. This indicates that the four metabolites were isomers.

M5, which eluted out at 13.4 min, was characterized by monitoring precursor/product ion pair *m/z* 271/197 (Fig. 5B). The value of its protonated molecule (*m/z* 271) was 14 Da lower than that of physcion. The fragment ions at *m/z* 169, 197, and 225 were derived from parent fragmentation of *m/z* 183 ($[MH\text{-}H_2O\text{-}3CO]^+$), 211 ($[MH\text{-}H_2O\text{-}2CO]^+$), 239 ($[MH\text{-}H_2O\text{-}CO]^+$), respectively (Fig. 5F). This suggests that M5 was the *O*-demethylation metabolite of physcion.

The formation of M6 was monitored by acquiring ion pair of *m/z* 462→333 (Fig. 6B). The MS/MS spectrum of M6 (Rt = 10.7 min) demonstrated the major fragment ions associated with cleavage of the NAC moiety (Fig. 6F). The product ion at *m/z* 130 corresponded to NAC moiety without the sulfur, and the fragment ion at *m/z* 162 was derived from NAC moiety with the sulfur. The product ion at *m/z* 333 was associated with the characteristic neutral loss of 129 Da from NAC conjugate M6. Since the molecular weight of NAC is 163 Da, the observed molecular ion of *m/z* 462

suggests that M6 resulted from a hydroxylation metabolite of physcion conjugated with a molecule of NAC.

M7 and M8 eluted out at 11.8 and 12.1 min respectively, showing their molecular ions at *m/z* 446 (Fig. 7B). The MS/MS spectra of M7 and M8 were acquired by MRM-EPI scanning (ion transition *m/z* 446/315) which displayed characteristic fragment ions of *m/z* 130, 162, 315, and 317 (Fig. 8B, 8C). Similarly, the product ion at *m/z* 130 corresponded to NAC moiety without the sulfur, and the fragment ion at *m/z* 162 was derived from NAC moiety with the sulfur. In addition, the product ion at *m/z* 317 matched the characteristic neutral loss of 129 Da for the NAC conjugates (M7 and M8). Therefore, M7 and M8 were isomers which shared the same molecular ions at *m/z* 446, possibly resulting from the parent compound conjugated with a molecule of NAC at two different positions.

Interestingly, we failed to detect M3 and M6 in HLM incubations which were conducted under similar condition as that of RLM incubations (Fig. 9).

Chemical Synthesis of Metabolites of Physcion. Chemical synthesis was carried out to verify the structure of M1–M8 obtained from the microsomal incubations above. Physcion oxidized in a series of chemical reactions with CrO_3 and borane-methylsulfide complex to acquire a product which revealed the same chromatographic and mass spectral behaviors as that of M1 formed in RLM incubations (Fig. 3A, S1A). Since the oxidation protocol was reported to selectively hydroxylate the benzylic carbon,[31] we proposed that M1 was 6-hydroxyphyscion.

Similarly, hydroxylation of physcion in oleum and boric acid also got an outcome in which the product had the same chromatographic and mass spectral behaviors as that of M2 produced in the RLM incubations (Fig. 3B, S1C). Besides, treatment of physcion with persulfate in sulfuric acid generated two products which had the same chromatographic and mass spectral behaviors as that of M3 and M4 generated in the RLM incubations (Fig. 4A, S2A, S2C). M3 was purified and characterized by LC-Q-TOF MS analysis (Table 1) and NMR. Three aromatic proton resonances were observed at 7.11, 7.34, and 7.49 ppm responsible for the protons at C-7, C-4 and C-5. However, no proton resonance was found to be responsible for the proton at C-2. This made us conclude that hydroxylation occurred at C-2. Together, the synthetic work allowed us to assign M3 as 2-hydroxyphyscion. The LC-Q-TOF MS data of M4 (Table 1) revealed the molecular ion which match the molecular formula ($C_{16}H_{12}O_6$) responsible for hydroxylated physcion.

The structure of M5 was verified by comparing its chromatographic and mass spectral properties with that of authentic standard emodin. As expected, M5 was identified as emodin (Fig. 5C, 5H).

In order to determine the source of M6, synthetic M1, M2, M3 and M4 were individually incubated with NAC in RLMs. M4-NAC reaction generated a product sharing the same chromatographic and mass spectral identities as those of M6 produced in microsomal incubations (Fig. 6C, 6H). Hence, M6 originated from M4 conjugated with a molecule of NAC.

Direct mixing of physcion with NAC in PBS buffer generated two products

which revealed the same chromatographic and mass spectral behaviors as those of M7 and M8 produced in the RLM incubations (Fig. 8A, S3A, S3C). M7 and M8 were then purified and characterized by LC-Q-TOF MS (Table 1) and NMR. Figure S4 shows the HMBC (long-range proton-carbon heteronuclear multiple bond correlation) spectrum of M7. Three aromatic proton resonances at 7.19, 7.27, and 7.52 ppm are responsible for the protons at C-7, C-4 and C-5. Carbon signals at δC21.50, 110.60, 113.60, 120.40, 124.40 and 181.5 ppm corresponded to C-11, C-9a, C-8a, C-5, C-7 and C-10, respectively. Additionally, the HMBC spectrum revealed that C-9a and C-10 had correlations with the proton at 7.27 ppm; C-8a, C-7, and C-10 had correlations with the proton at 7.52 ppm; C-11, C-5, and C-8a had correlations with the proton at 7.19 ppm. The NMR spectrum suggests that NAC is attached to C-2 of physcion.

The ^{1}H-NMR spectrum of M8 showed three aromatic proton resonances at 6.87, 7.18, and 7.53 ppm responsible for the protons at C-2, C-4 and C-5. Apparently, no proton resonance responded to the proton at C-7. This made us conclude that M8 was NAC conjugation took place at C-7 of physcion.

Metabolism of Physcion in Rats. *In vivo* metabolism of physcion was investigated by analyzing urine samples of rats with or without treatment of physcion. M1-M8 were found in the urine of the animals treated with physcion, and no such metabolites were observed in the control urine samples (Fig. 2C, 2D, 5D, 5E, 6D, 6E, 7C, 7D). The chromatographic and mass spectral behaviors of the metabolites detected in the

urine were in agreement with those produced in microsomal incubations (Fig. 2D, S1B, S1D, S2B, S2D, 5E, 5G, 6E, 6G, 7D, S3B, S3D).

P450 Enzymes Involved in Physcion Biotransformation. Recombinant human P450s were used to determine which P450 enzymes were responsible for the metabolism of physcion. Nine human recombinant P450 enzymes were individually incubated with physcion and NAC, and the formation of M1-M2, and M4-M5 was monitored to determine the specific P450 enzymes involved in the biotransformation of physcion (Fig. 10). P450 1A2 was found to be the major enzyme contributing to the production of M1. P450 2C19 was the primary enzyme participating in the generation of M2. The formation of M4 was catalyzed by P450 2C19 and then 3A4. P450 2B6 was the major enzyme catalyzing the formation of M5, followed by P450s 1A2 and 2C19. However, M3 and M6 were not found in recombinant human P450 incubations.

DISCUSSION

Physcion is a bioactive component in PMR which has been widely consumed in China and North America. However, studies also showed multiple adverse effects during its clinical trials, such as hepatotoxicity of PMR, but the mechanisms of the toxicities remain unknown. Investigation of metabolism pathways of physcion would be helpful for the understanding of the mechanisms of physcion toxic action. Firstly, we studied the mass spectrometric behavior and fragmentation pattern of physcion (Fig. 1), which would help the structural characterization of physcion metabolites. Whereafter, RLM incubations were conducted with physcion, using NAC as the capture reagent. Comparison of the changes in molecular masses (ΔM) and MS^2 spectral patterns of metabolites with that of parent drug could assist us to better characterize the metabolites. Four hydroxylation metabolites (M1−M4) (Fig. 2B), one *O*-demethylation metabolite (M5) (Fig. 5B), and three NAC conjugates (M6–M8) were detected by LC-MS/MS (Fig. 6B, 7B). Apparently, M1 was found to be the primary metabolite among the four hydroxylation metabolites (M1−M4) (Fig. S5), based on their relative abundance obtained from LC-MS/MS data. Interestingly, the metabolism of physcion showed some species difference. No M3, along with significantly decreased formation of M2/M4, was detected in the HLM incubations (Fig. 9) conducted under similar condition as RLM incubations. Besides, no M6 was found in the HLM incubations, possibly resulting from the decreased generation of M2/M4.

Chemical synthesis was carried out to verify the metabolites. M1 was

synthesized by hydroxylation of the benzylic carbon of physcion using CrO_3 and borane-methylsulfide complex (Fig. 3A). M2 was prepared by hydroxylation of physcion in oleum and boric acid (Fig. 3B). M3 and M4 were obtained from treatment of physcion with persulfate in sulfuric acid (Fig. 4A). The NMR spectrum demonstrated that M3 was 2-hydroxyphyscion. Unfortunately, we failed to obtain the NMR data of M1, M2 and M4, due to the lower yield and instability of the products. M5 was identified as emodin using the authentic compound (Fig. 5C, 5H). The mass spectrum of M6 suggests the metabolite was a NAC conjugate derived from hydroxylation metabolites of physcion. The origin of M6 was determined by incubation of individual synthetic M1, M2, M3 and M4 in RLM fortified with NAC. The result demonstrated M6 was derived from M4 conjugated with a molecule of NAC (Fig. 6C, 6H).

M7 and M8 were isomers resulting from direct reaction of physcion with NAC. We detected M7 and M8 in both RLM and HLM incubations with or without NADPH (Fig. 7A, 7B, 9E, 9F). This suggests that the formation of M7 and M8 was independent on P450 enzymes. The two metabolites were generated by direct adduction, followed by auto-oxidation possibly mediated by air. Additionally, the presence of NADPH was found to attenuate the formation of the two conjugates (Fig. 7A, 7B, 9E, 9F). This may explain that NADPH initiated P450-mediated oxidative metabolism of physcion and made physcion less available for the formation of M7 and M8. The NMR data showed that M7 was the conjugate with an NAC attached to C-2 of physcion (Fig. S4), while M8 was the adduct with an NAC conjugated at

C-7.

Metabolism of physcion *in vivo* was investigated by analyzing the urine samples of rats treated with physcion. As expected, M1-M8 were detected in the urine, and the urinary metabolites illustrated similar retention time and mass spectral fragment patterns with those of the corresponding metabolites produced in RLM incubations (Fig.2D, S1B, S1D, S2B, S2D, 5E, 5G, 6E, 6G, 7D, S3B, S3D).

Proposed metabolic pathways of physcion are displayed in Scheme 1. *O*-demethylation of physcion generated M5 which is emodin, a major AQ derivative found in PMR. Our previous work demonstrated that emodin was chemically reactive to thiol-containing agents.[34] Studies showed that emodin could cause a variety of toxic effects such as nephrotoxicity,[35] genotoxicity[36] and hepatotoxicity.[37] Hence, emodin, as metabolite of physcion, might contribute to physcion-induced hepatocyte toxicity.

In conclusion, five oxidative metabolites (M1−M5) of physcion and three related NAC conjugates (M6–M8) were detected in RLM incubations and in urine samples of rats after exposure to physcion, while HLM incubations produced four oxidative metabolites and two NAC conjugates. P450 1A2, 2C19 and 2B6 were the primary enzymes mediating the hydroxylation of physcion. The parent compound and all oxidative metabolites showed electrophilicity. The metabolism work would allow us to better understand the molecular mechanisms of physcion-induced hepatotoxicity.

Author Contributions

The manuscript was written by Jiang Zheng and Xiaotong Qin. The research design was performed by Jiang Zheng and Ying Peng. Experiments were performed and data analysis by Xiaotong Qin.

Funding sources

This work was supported in part by the National Natural Science Foundation of China (No. 81430086, 81373471 and 81773813).

Supporting Information Available

MS/MS spectra of M1-M4 and M7-M8 generated in chemical synthesis and found in urine samples of rats treated with physcion were supplied as supporting information. HMBC (long-range proton-carbon heteronuclear multiple bond correlation) spectrum of M7 was also provided, along with the relative abundance of metabolites (M1-M8) obtained from LC-MS/MS analysis of RLM incubations containing physcion in the presence of NADPH. This material can be accessed via the Internet at http://pubs.acs.org.

Notes

The authors declare no competing financial interest.

Abbreviations: CE, collision energy; DMSO, dimethyl sulfoxide; DP, declustering potential; EPI, enhanced product ion; HMBC, long-range protoncarbon heteronuclear multiple bond correlation; IDA, information-dependent acquisition; LC-MS/MS, liquid chromatography-tandem mass spectrometry; MRM, multiple-reaction monitoring; NAC, *N*-acetyl cysteine; NADPH, *β*-nicotinamide adenine dinucleotide 2′-phosphate reduced tetrasodium salt; NMR, nuclear magnetic resonance; PMR, Polygoni Multiflori Radix; THF, tetrahydrofuran.

References

(1) Lv, L., Shao, X., Wang, L., Huang, D., Ho, C. T., and Sang, S. (2010) Stilbene glucoside from *Polygonum multiflorum* Thunb.: a novel natural inhibitor of advanced glycation end product formation by trapping of methylglyoxal. *J. Agric. Food Chem*. *58,* 2239–2245.

(2) Lin, L., Ni, B., Lin, H., Zhang, M., Li, X., Yin, X., Qu, C., and Ni, J. (2015) Traditional usages, botany, phytochemistry, pharmacology and toxicology of *Polygonum multiflorum* Thumb.: a review. *J. Ethnopharmacol*. *159,* 158–183.

(3) Bounda, G. A., and Feng, Y. U. (2015) Review of clinical studies of *Polygonum multiflorum* Thunb. and its isolated bioactive compounds. *Pharmacogn. Res*. *7,* 225–236.

(4) Wang, T. H., Zhang, J., Qiu, X. H., Bai, J. Q., Gao, Y. H., and Xu, W. (2016) Application of ultra-high-performance liquid chromatography coupled with LTQ-Orbitrap mass spectrometry for the qualitative and quantitative analysis of *Polygonum multiflorum* Thumb. and its processed products. *Molecules*. *21,* 40.

(5) Singh, R., Geetanjali, Chauhan, S. M. (2004) 9,10-Anthraquinones and other biologically active compounds from the genus Rubia. *Chem*. *Biodivers*. *1,* 1241–1264.

(6) Niu, J. H. (1996) A severe liver damage case induced by Shou Wu Pian though oral administration. *Chin*. *J. New Drugs Clin*. *Rem*. *15,* 382.

(7) Ye, Q. H. (1996) An acute toxic hepatopathy case induced by Radix Polygoni Multiflori. *Chin*. *J. Integr*. *Med*. *16,* 732.

(8) Sun, J. (2002) A severe liver damage case induced by tonic traditional Chinese medicine for many times. *Chin*. *J. Integr*. *Tradit*. *West*. *Med*. *10,* 292.

(9) Zhao, X. D. (2007) An liver damage case induced by Shou Wu Wan. *China J. Chin*. *Mater*. *Med*. *32,* 444.

(10) But, P. P., Tomlinson, B., and Lee, K. L. (1996) Hepatitis related to the Chinese medicine Shou-wu-pian manufactured from *Polygonum multiflorum*. *Vet*. *Hum*. *Toxicol*. *38,* 280–282.

(11) Park, G. J., Mann, S. P., and Ngu, M. C. (2001) Acute hepatitis induced by Shou-Wu-Pian, a herbal product derived from *Polygonum multiflorum*. *J. Gastroen*. *Hepatol*. *16,* 115–117.

(12) Battinelli, L., Daniele, C., and Mazzanti, G. (2004) New case of acute hepatitis following the consumption of Shou Wu Pian, a Chinese herbal product derived from *Polygonum multiflorum*. *Ann*. *Intern*. *Med*. *140,* W30.

(13) Panis, B., Wong, D. R., Hooymans, P. M., De, Smet. P. A., and Rosias, P. P. (2005) Recurrent toxic hepatitis in a Caucasian girl related to the use of Shou-Wu-Pian, a Chinese herbal preparation. *J*. *Pediatr*. *Gastroenterol*. *Nutr*. *41,* 256–258.

(14) Cárdenas, A., Restrepo, J. C., and Sierra, F. (2006) Acute hepatitis due to shen-min: a herbal product derived from *Polygonum multiflorum*. *J*. *Clin*. *Gastroenterol*. *40,* 629–632.

(15) Yuen, M. F., Tam, S., Fung, J., Wong, D. K., Wong, B. C., and Lai, C. L. (2006) Traditional Chinese medicine causing hepatotoxicity in patients with chronic hepatitis B infection: a 1-year prospective study. *Aliment*. *Pharmacol*. *Ther*. *24,* 1179–1186.

(16) Min, H. J., Jung, K. A., Kim, H. J., Kim, T. H., Jung, W. T., Lee, O. K., and Lee, J. S. (2008) Twelve cases of toxic hepatitis related to the root of *Polygonum multiflorum* Thunb.. *J*. *Hepatol*. *48,* S356.

(17) Cho, H. C., Min, H. J., Ha, C. Y., Kim, H. J., Kim, T. H., Jung, W. T., Lee, O. J., and Bae, I. G. (2009) Reactivation of pulmonary tuberculosis in a patient with *Polygonum multiflorum* Thunb-induced hepatitis. *Gut Liver 3,* 52–56.

(18) Navarro, V. J., and Senior, J. R. (2006) Drug-related hepatotoxicity. *N*. *Engl*. *J*. *Med*. *354,* 731–739.

(19) Murray, K. F., Hadzic, N., Wirth, S., Bassett, M. and Kelly, D. (2008) Drug-related hepatotoxicity and acute liver failure. *J*. *Pediatr*. *Gastroenterol*. *Nutr*. *47,* 395–405.

(20) Vanderperren, B., Rizzo, M., Angenot, L., Haufroid, V., Jadoul, M., and

Hantson, P. (2005) Acute liver failure with renal impairment related to the abuse of senna anthraquinone glycosides. *Ann. Pharmacother. 39,* 1353–1357.

(21) Wang, J., Zhao, Y., Xiao, X., Li, H., Zhao, H., Zhang, P., and Jin, C. (2009) Assessment of them renal protection and hepatotoxicity of rhubarb extract in rats. *J. Ethnopharmacol. 124,* 18–25.

(22) Agarwal, S. K., Singh, S. S., Verma, S., and Kumar, S. (2000) Antifungal activity of anthraquinone derivatives from Rheum emodi. *J. Ethnopharmacol. 72,* 43–46.

(23) Anke, H., Kolthoum, I., Zahner, H., and Laatsch, H. (1980) Metabolic products of microorganisms. 185. The anthraquinones of the Aspergillus glaucus group. I. Occurrence, isolation, identification and antimicrobial activity. *Arch. Microbiol. 126,* 223–230.

(24) Smetania, O. F., Kalinovsky, A. I., Khudyakova, Y. V., Pivkin, M. V., Dmitrenok, P. S., Fedorov, S. N., Ji, H., Kwak, J. Y., and Kuznetsova, T. A. (2007) Indole alkaloids produced by a marine fungus isolate of Penicillium janthinellum Biourge. *J. Nat. Prod. 70,* 906–909.

(25) Ghosh, S., Das, Sarma. M., Patra, A., and Hazra, B. (2010) Anti-inflammatory and anticancer compounds isolated from Ventilago madraspatana Gaertn., Rubia cordifolia Linn. and Lantana camara Linn. *J. Pharm. Pharmacol. 62,* 1158–1166.

(26) Tamokou, Jde. D., Tala, M. F., Wabo, H. K., Kuiate, J. R., and Tane, P. (2009) Antimicrobial activities of methanol extract and compounds from stem bark of Vismia rubescens. *J. Ethnopharmacol. 124,* 571–575.

(27) Pecere, T., Gazzola, M. V., Mucignat, C., Parolin, C., Vecchia, F. D., Cavaggioni, A., Basso. G., Diaspro, A., Salvato, B., Carli, M., and Palu, G. (2000) Aloe-emodin is a new type of anticancer agent with selective activity against neuroectodermal tumors. *Cancer Res. 60,* 2800–2804.

(28) Koyama, J., Morita, I., Tagahara, K., Ogata, M., Mukainaka, T., Tokuda, H., and Nishino, H. (2001) Inhibitory effects of anthraquinones and

bianthraquinones on Epstein–Barr virus activation. *Cancer Lett. 170,* 15–18.

(29) Kuete, V., Wabo, H. K., Eyong, K. O., Feussi, M. T., Wiench, B., Krusche, B., Tane, P., Folefoc, G. N., and Efferth, T. (2011) Anticancer activities of six selected natural compounds of some Cameroonian medicinal plants. *PLoS. One. 6,* e21762.

(30) Lin, D., Li, C., Peng, Y., Gao, H., and Zheng, J. (2014) Cytochrome p450-mediated metabolic activation of diosbulbin B. *Drug Metab. Dispos. 42,* 1727–1736.

(31) Morooka, N., Itoi, N., and Y, Ueno. (1986) Identification and mutagenicity of the metabofites of emodin in hepatic microsomes of rats. *Ann. Meet. Jpn. Soc. Agric. Chem., Abstract p*. 409.

(32) Banks, H. J., Cameron, D. W., and Raverty, W. D. (1978) Hydroxylation of anthraquinones in oleum and in sulfuric acid. *Aust. J. Chem. 31,* 2271-2282.

(33) Rodrigues, A. D. (1999) Integrated cytochrome P450 reaction phenotyping: attempting to bridge the gap between cDNA-expressed cytochromes P450 and native human liver microsomes. *Biochem. Pharmacol. 57,* 465-480.

(34) Qin, B., Xu, Y., Chen, J., Huang, W., Peng, Y., and Zheng, J. (2016) Chemical reactivity of emodin and its oxidative metabolites to thiols. *Chem. Res. Toxicol. 29,* 2114-2124.

(35) Wang, C., Jiang, Z., Yao, J., Wu, X., Sun, L., Liu, C., Duan, W., Yan, M., Sun, L., Liu, J., and Zhang, L. (2008) Participation of cathepsin B in emodin-induced apoptosis in HK-2 Cells. *Toxicol. Lett. 181,* 196–204.

(36) Li, Y., Luan, Y., Qi, X., Li, M., Gong, L., Xue, X., Wu, X., Wu, Y., Chen, M., Xing, G., Yao, J., and Ren, J. (2010) Emodin triggers DNA double-strand breaks by stabilizing topoisomerase II-DNA cleavage complexes and by inhibiting ATP hydrolysis of topoisomerase II. *Toxicol. Sci. 118,* 435–443.

(37) Li, C. L., Ma, J., Zheng, L., Li, H. J., and Li, P. (2012) Determination of emodin in L-02 cells and cell culture media with liquid chromatography–mass

spectrometry: application to a cellular toxicokinetic study. *J. Pharm. Biomed. Anal. 71,* 71–78.

Figure Legends

Figure 1. MS/MS spectrum of physcion.

Figure 2. Chromatograms of M1, M2, M3 and M4. Extracted ion (*m/z* 301/199 for M1, M2, M3 and M4) chromatograms obtained from LC-MS/MS analysis of RLM incubations containing physcion in the absence (**A**) or presence (**B**) of NADPH. Extracted ion (*m/z* 301/199 for M1, M2, M3 and M4) chromatograms obtained from LC-MS/MS analysis of urine samples of rats treated with vehicle (**C**) or physcion (**D**).

Figure 3. Characterization of M1 and M2. Extracted ion (*m/z* 301/199) chromatograms obtained from LC-MS/MS analysis of synthetic M1 (**A**) and synthetic M2 (B). MS/MS spectra of M1 generated in RLM incubations (**C**) and MS/MS spectra of M2 generated in RLM incubations (**D**).

Figure 4. Characterization of M3 and M4. **A**: Extracted ion (*m/z* 301/199) chromatogram obtained from LC-MS/MS analysis of synthetic M3 and M4. MS/MS spectra of M3 generated in RLM incubations (**B**) and MS/MS spectra of M4 generated in RLM incubations (**C**).

Figure 5. Characterization of M5. Extracted ion (*m/z* 271/197) chromatograms obtained from LC-MS/MS analysis of RLM incubations containing physcion in the absence (**A**) or presence (**B**) of NADPH. (**C**) Extracted ion (*m/z* 271/199) chromatogram obtained from LC-MS/MS analysis of chemistry reference substance of emodin. Extracted ion (*m/z* 271→197, M5) chromatograms obtained from

LC-MS/MS analysis of the urine samples of rats after (**E**) and before (**D**) treatment with physcion. MS/MS spectra of M5 generated in RLM incubations (**F**), and found in urine samples of rats treated with physcion (**G**) and chemistry reference substance of emodin (**H**).

Figure 6. Characterization of M6. Extracted ion (*m/z* 462/333) chromatograms obtained from LC-MS/MS analysis of RLM incubations containing physcion in the absence (**A**) or presence (**B**) of NADPH. (**C**) Extracted ion (*m/z* 462/333) chromatogram obtained from LC-MS/MS analysis of microsome incubations of synthetic M4 with RLM, NADPH, and NAC. Extracted ion (*m/z* 462→333) chromatograms obtained from LC-MS/MS analysis of the urine samples of rats after (**E**) and before (**D**) treatment with physcion. MS/MS spectra of M6 generated in RLM incubations (**F**), and found in urine samples of rats treated with physcion (**G**) and microsome incubations of synthetic M4 with RLM, NADPH, and NAC (**H**).

Figure 7. Chromatograms of M7 and M8. Extracted ion (*m*/*z* 446/315 for M7 and M8) chromatograms obtained from LC-MS/MS analysis of RLM incubations containing physcion in the absence (**A**) or presence (**B**) of NADPH. Extracted ion (*m*/*z* 446/315 for M7 and M8) chromatograms obtained from LC-MS/MS analysis of urine samples of rats treated with vehicle (**C**) or physcion (**D**).

Figure 8. Characterization of M7 and M8. **A**: Extracted ion (*m*/*z* 446/315) chromatogram obtained from LC-MS/MS analysis of synthetic M7 and M8. MS/MS spectra of M7 generated in RLM incubations (**B**) and MS/MS spectra of M8

generated in RLM incubations (**C**).

Figure 9. Metabolite profile of HLM incubations. Extracted ion (*m/z* 301/199 for M1, M2 and M4) chromatograms obtained from LC-MS/MS analysis of HLM incubations containing physcion in the absence (**A**) or presence (**B**) of NADPH. Extracted ion (*m/z* 271/197 for M5) chromatograms obtained from LC-MS/MS analysis of HLM incubations containing physcion in the absence (**C**) or presence (**D**) of NADPH. Extracted ion (*m/z* 446/315 for M7 and M8) chromatograms obtained from LC-MS/MS analysis of HLM incubations containing physcion in the absence (**E**) or presence (**F**) of NADPH.

Figure 10. Individual human recombinant P450 enzymes involved in hydroxylation of Physcion. Physcion was incubated with individual human recombinant P450 enzymes. The catalytic capabilities of the enzymes were evaluated by monitoring the formation of M1-M2 and M4-M5 after normalization based on the relative content of the corresponding P450 enzymes in human liver microsomes. Data represent the mean ± S.D. (n = 3)

Scheme Legend

Scheme 1. Proposed pathways for the formation of hydroxylation metabolites of physcion and related NAC adducts.

Table Legend

Table 1. Mass spectrometric profiling data obtained from LC-Q-TOF MS analyses of synthetic M3, M4, M7 and M8.

Figure 1

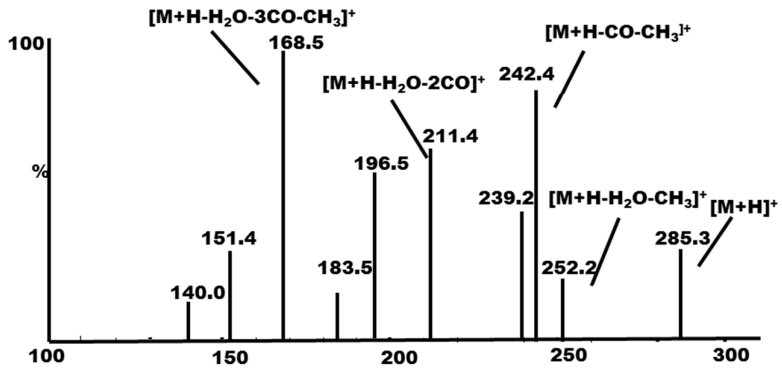
[M+H-H2O-3CO-CH3]+
168.5
[M+H-CO-CH3]+
242.4
[M+H-H2O-2CO]+
211.4
196.5
100
%
239.2
[M+H-H2O-CH3]+
[M+H]+
285.3
151.4
183.5
252.2
140.0
100
150
200
250
300

Figure 2

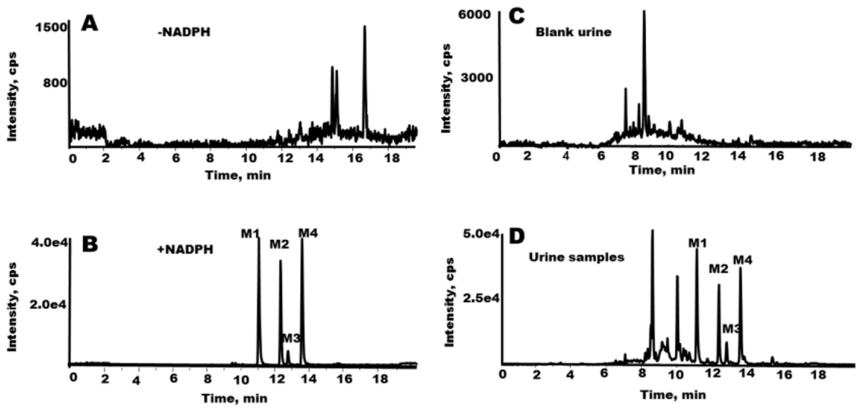
A
-NADPH
1500
800
Intensity, cps
Time, min
C
Blank urine
6000
3000
B
+NADPH
M1
M2
M3
M4
4.0e4
2.0e4
D
Urine samples
5.0e4
2.5e4

Figure 3

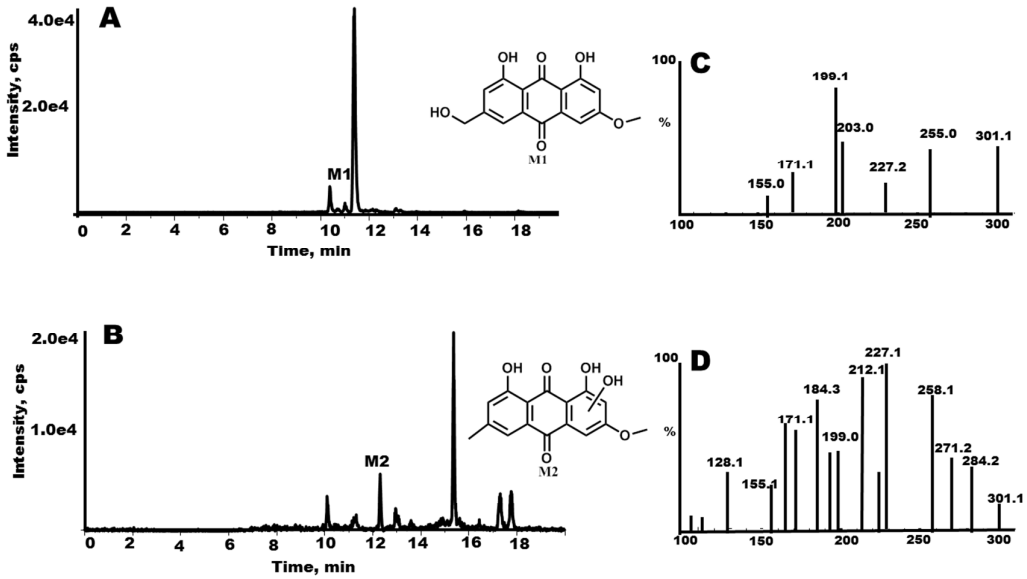
A
4.0e4
2.0e4
Intensity, cps
M1
0 2 4 6 8 10 12 14 16 18
Time, min
OH O OH
HO
O
O
M1
C
100
%
199.1
203.0
255.0
301.1
171.1
227.2
155.0
100 150 200 250 300
B
2.0e4
1.0e4
Intensity, cps
M2
0 2 4 6 8 10 12 14 16 18
Time, min
OH O OH OH
O
O
M2
D
100
%
227.1
212.1
184.3
258.1
171.1
199.0
271.2
128.1
284.2
155.1
301.1
100 150 200 250 300

Figure 4

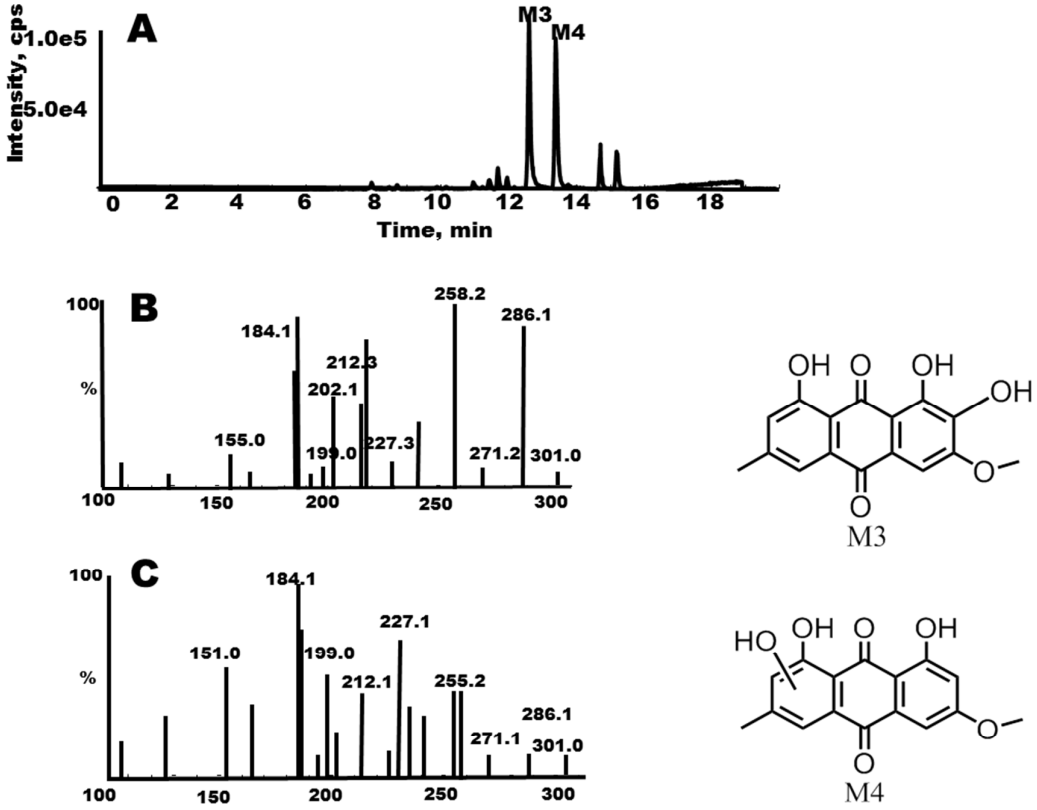
A
Intensity, cps
1.0e5
5.0e4
M3
M4
0 2 4 6 8 10 12 14 16 18
Time, min
B
100
%
184.1
212.3
202.1
155.0
199.0
227.3
258.2
286.1
271.2
301.0
100 150 200 250 300
C
100
%
184.1
227.1
151.0
199.0
212.1
255.2
286.1
271.1
301.0
100 150 200 250 300
OH O OH OH
O
O
M3
HO OH O OH
O
O
M4

Figure 5

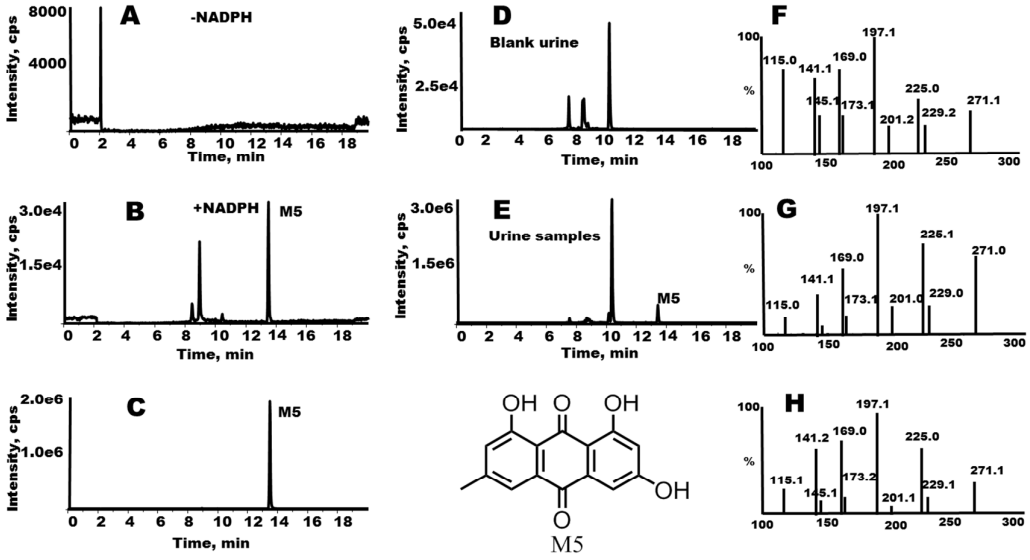
A
-NADPH
Intensity, cps
8000
4000
Time, min
B
+NADPH
M5
3.0e4
1.5e4
C
2.0e6
1.0e6
D
Blank urine
5.0e4
2.5e4
E
Urine samples
3.0e6
1.5e6
F
G
H
M5

Figure 6

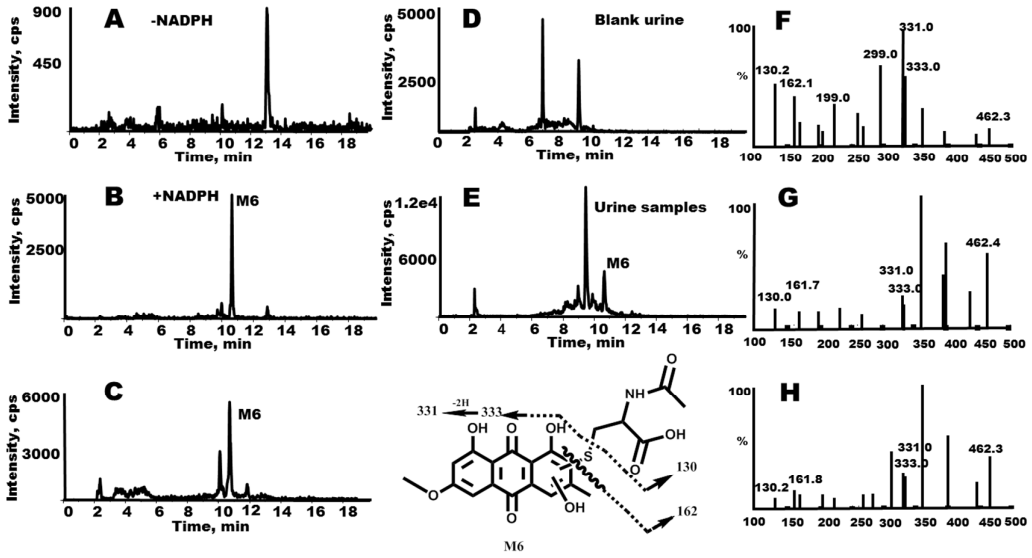
A
-NADPH
B
+NADPH
M6
C
M6
D
Blank urine
E
Urine samples
M6
F
G
H
Intensity, cps
Time, min
331
-2H
333
OH
O
NH
S
130
162
M6

Figure 7

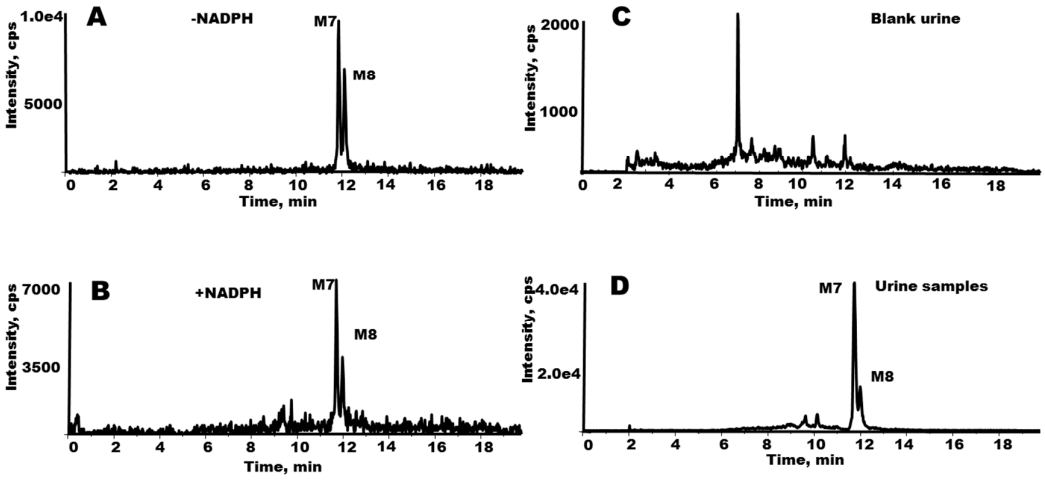
A
-NADPH
M7
M8
1.0e4
5000
Intensity, cps
Time, min
B
+NADPH
M7
M8
7000
3500
Intensity, cps
Time, min
C
Blank urine
2000
1000
Intensity, cps
Time, min
D
Urine samples
M7
M8
4.0e4
2.0e4
Intensity, cps
Time, min

Figure 8

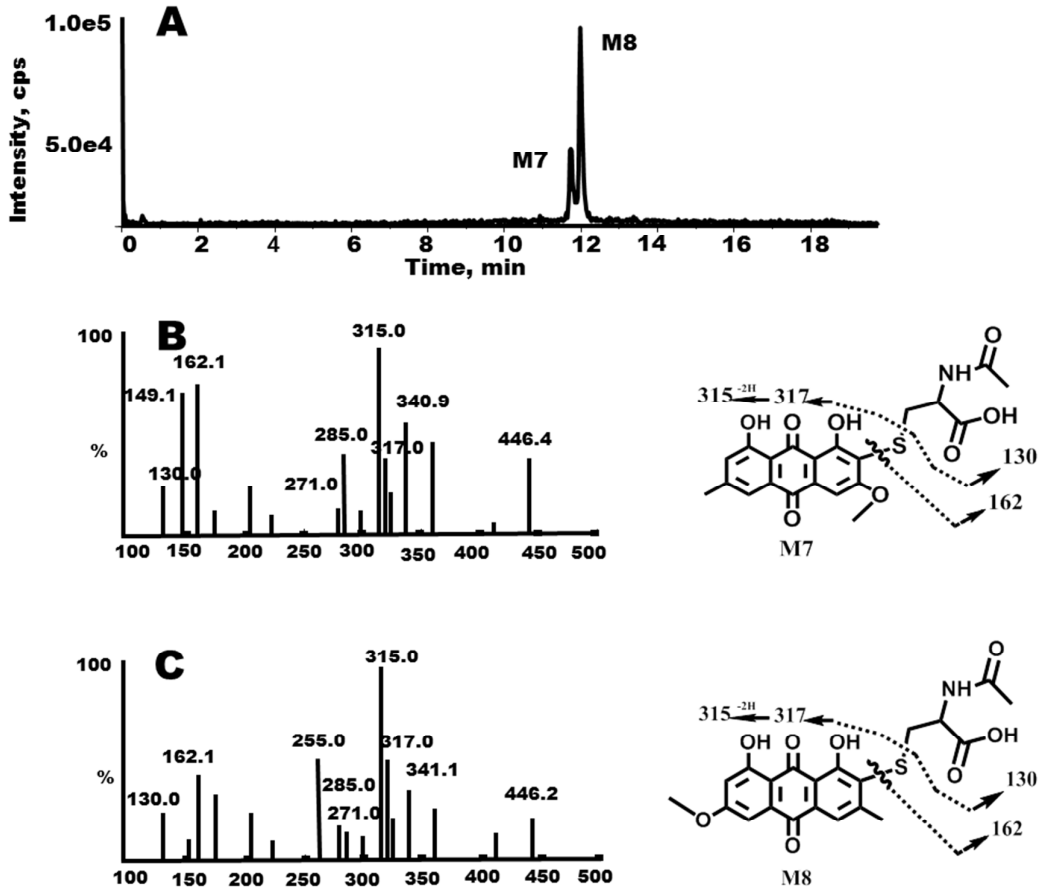
A
1.0e5
5.0e4
Intensity, cps
M8
M7
0 2 4 6 8 10 12 14 16 18
Time, min
B
100
%
315.0
162.1
149.1
340.9
285.0
317.0
446.4
130.0
271.0
100 150 200 250 300 350 400 450 500
315-2H
317
NH
OH
O
S
130
162
M7
C
100
%
315.0
255.0
317.0
162.1
341.1
285.0
446.2
130.0
271.0
100 150 200 250 300 350 400 450 500
315-2H
317
NH
OH
O
S
130
162
M8

Figure 9

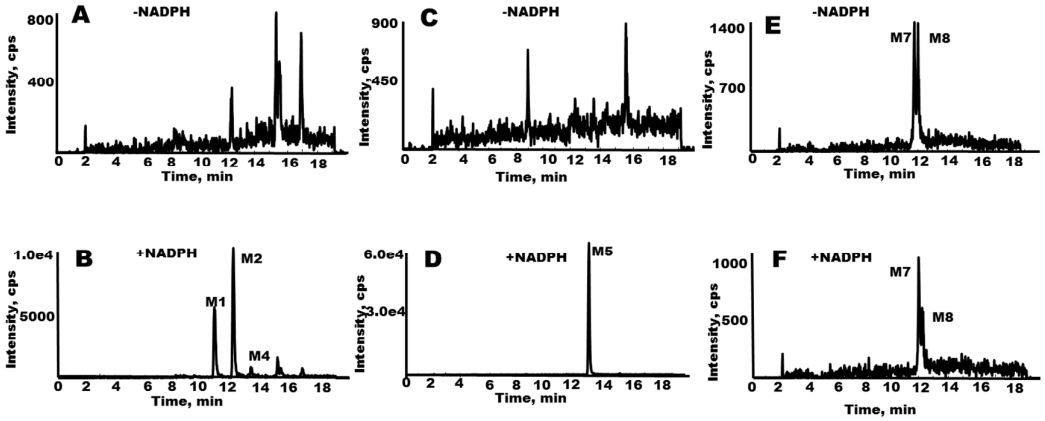
A
-NADPH
800
400
Intensity, cps
0 2 4 6 8 10 12 14 16 18
Time, min
C
-NADPH
900
450
Intensity, cps
0 2 4 6 8 10 12 14 16 18
Time, min
E
-NADPH
M7
M8
1400
700
Intensity, cps
0 2 4 6 8 10 12 14 16 18
Time, min
B
+NADPH
M2
M1
M4
1.0e4
5000
Intensity, cps
0 2 4 6 8 10 12 14 16 18
Time, min
D
+NADPH
M5
6.0e4
3.0e4
Intensity, cps
0 2 4 6 8 10 12 14 16 18
Time, min
F
+NADPH
M7
M8
1000
500
Intensity, cps
0 2 4 6 8 10 12 14 16 18
Time, min

Figure 10

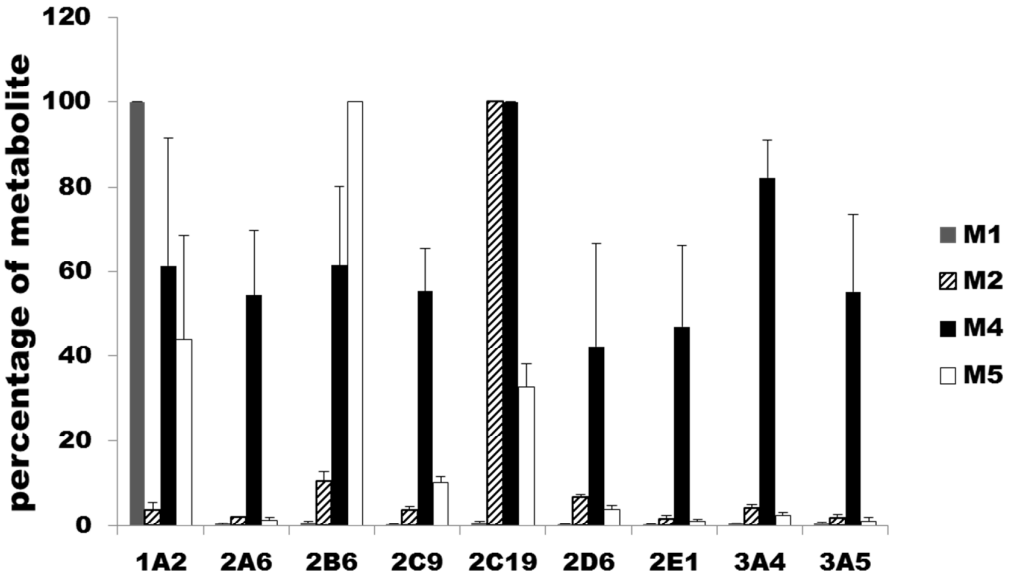
percentage of metabolite
120
100
80
60
40
20
0
1A2
2A6
2B6
2C9
2C19
2D6
2E1
3A4
3A5
M1
M2
M4
M5

Scheme 1

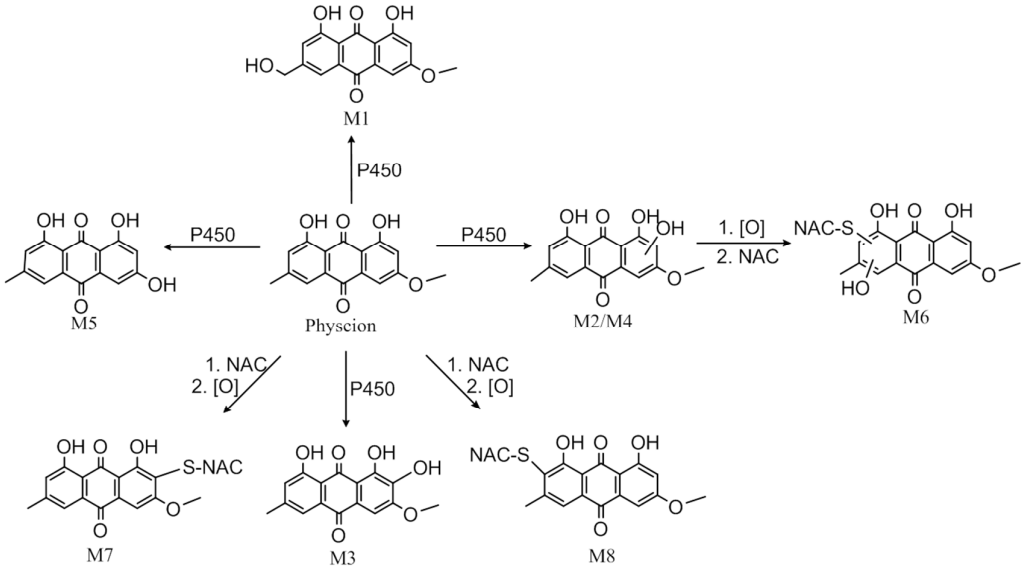
M1
P450
M5
P450
Physcion
P450
M2/M4
1. [O]
2. NAC
M6
1. NAC
2. [O]
P450
1. NAC
2. [O]
M7
M3
M8

Table 1

		$[M+Na]^+$		error		
compound	formula	calculated	detected	ppm	mDa	sigma
M3	$C_{16}H_{12}NaO_6$	323.0526	323.0522	1.3	0.41	0.03416
M4	$C_{16}H_{12}NaO_6$	323.0526	323.0527	-0.2	-0.07	0.01048
M7	$C_{21}H_{19}NNaO_8S$	468.0724	468.0717	1.3	0.63	0.00884
M8	$C_{21}H_{19}NNaO_8S$	468.0724	468.0719	0.9	0.43	0.01162